HAL
open science

Hydration of tricalcium silicate (C 3 S) at high temperature and high pressure

B. Bresson, Fabienne Meducin, H. Zanni, C. Noïk

To cite this version:

B. Bresson, Fabienne Meducin, H. Zanni, C. Noïk. Hydration of tricalcium silicate (C 3 S) at high temperature and high pressure. Journal of Materials Science, 2002, 37 (24), pp.5355-5365. 10.1023/A:1021093528888 . hal-02362428

HAL Id: hal-02362428

https://hal.science/hal-02362428v1

Submitted on 20 Jan 2021

HAL is a multi-disciplinary open access archive for the deposit and dissemination of scientific research documents, whether they are published or not. The documents may come from teaching and research institutions in France or abroad, or from public or private research centers.

L'archive ouverte pluridisciplinaire **HAL**, est destinée au dépôt et à la diffusion de documents scientifiques de niveau recherche, publiés ou non, émanant des établissements d'enseignement et de recherche français ou étrangers, des laboratoires publics ou privés.

Hydration of tricalcium silicate (C_3S) at high temperature and high pressure

B. BRESSON, F. MEDUCIN, H. ZANNI
Laboratoire de Physique et Mécanique des Milieux Hétérogènes, UMR CNRS 7636, ESPCI, 10 rue Vauquelin, 75005 Paris, France
E-mail: Bruno.Bresson@espci.fr

C. NOIK
Institut Français du Pétrole, 1-4 avenue de Bois Préau, 92506 Rueil-Malmaison, France

Hydration products of tricalcium silicate (C_3S) are the calcium silicate hydrates (C-S-H) and Portlandite. Silica fume, added to anhydrous cement in industrial formulations reacts with Portlandite and leads to C-S-H different from the previous one. C_3S hydration with and without silica fume has been studied under high pressure (1000 bar) and high temperature (160°C) by numerous techniques (^{29}Si and ^{1}H NMR, XRD, Thermal analysis, SEM) for different hydration times. In these conditions, high temperature more stable crystalline phases are formed and their kinetics of formation is dependent on pressure. Besides, electrical conductivity measurement on hydrating cement under pressure have been carried out in order to evidence the great dependence of hydration kinetics with pressure. This study proposes a practical phase diagram which allows on a thermodynamical base to understand the change of equilibrium temperature with pressure. The kinetics of reaction has been studied and mechanisms of reaction proposed to explain the results.
© *2002 Kluwer Academic Publishers*

1. Introduction

Tricalcium silicate (C_3S in cement chemist's notation: $C = CaO$, $S = SiO_2$, $H = H_2O$) is the major component of Portland cement used in oil wells cement formulation. At room temperature, the products formed during the C_3S hydration are the non stoichiometric and non crystalline calcium silicate hydrates C-S-H, and portlandite ($Ca(OH)_2$), which is a crystalline phase [1].

Oil wells cements experience high temperature (up to 250°C) and high pressure (up to 1000 bar) conditions and hydration products formed under these conditions are different from those obtained in normal conditions. In particular, C-S-H phase is no longer stable at high temperature [2]. Cement hydration at high temperature has been widely studied [3–5] but very few studies deal with pressure influence, which is of great importance in hydration [2, 6]. These studies are achieved in the system CaO-SiO_2-H_2O where equilibrium diagrams are drawn but no theoretical tool is introduced to explain the results. Moreover the main problem of a study in the CaO-SiO_2-H_2O system is due to great difficulty to reach and reverse equilibria [7, 8]. The time scale associated to the equilibrium can be a few years [9]. These diagrams are not adapted to a well understanding of early stage C_3S paste hydration at high temperature and under high pressure: α-C_2SH and C-S-H phases do not appear as equilibrium phases in these diagrams while being readily formed in early stages of hydration and of great importance in the material properties [3].

The equilibrium concept has to be precised by the time scale used and the study of equilibrium cannot be dissociated from a kinetics study [2]. In this study, the local equilibrium concept is used when the phase's rule is respected on a small volume (in 20 μm length cube). The time scale used is few hours up to few days typically so that intermediate metastable products as C-S-H or α-C_2SH can be considered as an equilibrium phase.

The aim of this work is to provide a useful tool for the description and understanding of the C_3S early stage hydration with and without ground quartz. A cell was especially designed to measure electrical conductivity during hydration under high pressure and high temperature. Electrical conductivity in cement hydrating pastes depends on the ionic concentration in the interstatial solution and on the connectivity of the network [10, 11]. This measurement is very useful to follow the time evolution of hydration, which depends a lot on pressure and temperature.

Hydrated samples were analysed by different techniques like Quantitative XRD, ^{29}Si and ^{1}H NMR, thermal analysis, which allow to build a phase diagram on thermodynamical basis useful to interpret results: displacement of equilibrium temperature can be explained with molar volume difference between phases in equilibrium. The study shows how kinetics of reaction and displacement of equilibrium temperature are closely related to temperature and pressure conditions.

2. Experimental procedure

2.1. Sample preparation

Anhydrous C_3S was supplied by Ciments Français-Italcementi and its structure checked by X-ray diffraction. Dowell ground quartz with a 15 μm granulometry was used. Two types of sample were prepared: C_3S hydrated with silica flour and C_3S hydrated without silica flour. The samples hydrated with silica flour were prepared with a silica-to-C_3S ratio equal to 0.4 and a water-to-solid weight ratio equal to 0.55. The samples hydrated without silica flour were prepared with a water-to-solid weight ratio equal to 0.44. The samples were synthesized at different temperatures and at a pressure ranging from atmospheric pressure to 1200 bar. Three studying temperatures were retained: room temperature, 120°C and 160°C.

The samples were prepared by mixing anhydrous product to desionized and boiled water. The paste was poured in a Teflon container then introduced in a especially designed high temperature and high pressure cell allowing *in situ* electrical conductivity measurement: two isolated electric wires go through the cell cap and are connected to electrodes embedded in the paste. The pressure was obtained by a high pressure inert gas generator and the temperature obtained by heating the cell with a collar surrounding the cell and connected to a power-regulated generator. The temperature was controlled by a thermocouple embedded in the paste within the cell and it did not vary of more than one degree. The pressure was controlled by a pressure captor directly connected to the cell. Just after mixing of anhydrous product to water, the sample was brought at the required pressure and then heated to the required temperature. The sampled were hydrated during a period from 15 hours typically to a few days. The hydration was then stopped by Acetone-Ether drying.

2.2. Experimental methods

A conductimeter (Tacussel CD 810) with a fixed chosen frequency allowed to do conductivity measurement. The cut-off frequency in the paste during the first stage of hydration was measured by drawing the imaginary part of conductivity versus real part: a frequency of 20 kHz was determined. It has been shown—by following the cut-off frequency—that this cut-off frequency does not change during the first stage of hydration. A frequency of 16 kHz (close to cut-off frequency of the paste) was chosen for the measurements with the conductimeter. The study does not take into account of the error, which can arise, from the real cut-off frequency and the fixed chosen measurement frequency.

Several experimental techniques were used to study the samples. Crystalline phases were analysed by X-ray diffraction used as a qualitative technique and as quantitative technique through Rietveld refinements. This well-known technique has already been used in cement application in order to extract quantitative results from XRD diagram [12, 13]. It is very useful in this case because all the structures needed are resolved in the literature and the treatment is quick [14–18]. The main difficulties when applying this technique in hydrated cements arise from the presence of a large amount of non-well crystallized phases as C-S-H mixed with other crystallized phases. The contribution of non-well crystallized phases in the diffractogram is a very broad peak, which can be included in the background. The background affected manually in order to simulate the diffractogram has a great influence on the final result and on the phases quantification. Moreover, the problem of preferred orientation could not be avoided for the portlandite phases. The results given by Rietveld method are used to estimate the amount of each phase in the final product and to make a comparison basis between each sample, which are always analysed in the same way.

The XRD sample was prepared by mixing the hydration products with α-corundun in a 50 : 50 ratio and grinding them together during twenty minutes. The diffractogram (obtained on a diffractometer Philips PW 170) was acquired between 7° and 85° with a step of 0.03° and an acquisition of 15 s per degree. The quantitative calculations are done in comparison with the weight of fully dried product: A part of the sample was analysed by thermal analysis at the same time as XRD acquisition in order to have the full amount of water of the sample.

The thermal analysis allows to have the weight loss for each phase in the sample analysed and then can be systematically compared with Rietveld results in order to check the amount of each phase, especially for the portlandite determination which must be corrected because of preferred orientation in XRD analysis. The analyses were carried out with a temperature increase of 10°C per minute between 25°C and 1050°C under N_2 circulation.

NMR, sensible to the local order, is a tool adapted to the study of non-well crystallized phases C-S-H with a structure based on SiO_4 chains with variable length [19]. ^{29}Si single pulse NMR spectra were analysed using the Q_n classification, where Q stands for SiO_4 tetrahedron and n refers to the number of tetrahedra linked by oxygen bonds to the previous tetrahedron. Q_2 is a middle chain site (linked to two tetrahedra), Q_1 is an end-chain site and Q_0 is a monomeric site. The peaks located between −65 ppm and −75 ppm correspond to a Q_0 entity, characteristic of C_3S anhydrous unreacted material and the peaks located around −80 ppm and −85 ppm correspond to Q_1 and Q_2 entities, characteristic of C-S-H or other phases as α-C_2SH or Jaffeite [20]. ^{1}H-^{29}Si cross polarization allows to enhance the signal of SiO_4 tetrahedra surrounded by ^{1}H proton via ^{1}H polarization transfer. We can vary the contact time between the two systems in order to have a dynamic of polarization characteristic.

^{1}H CRAMPS (Combined Rotation and MultiPulse Spectroscopy) has already been applied to C_3S hydration [21]. This technique allows to have high resolved ^{1}H NMR spectra in the hydration products. It is possible to distinguish in the spectra the ^{1}H lines corresponding to Ca—OH, Si—OH and H—OH groups and to estimate their populations, the CRAMPS technique being a quantitative technique. It had been shown on C_3S hydration at high temperature (120°C) that a great amount

of Ca—OH bound is present and that the C_3S hydration competes with pozzolanic reaction during hydration at 120°C. All the NMR experiments have been carried out on 500 MHz and 300 MHz Bruker spectrometers.

SEM was also used to observe the morphology and recognize the phases present in the system and confirm other results.

3. Results

3.1. Hydration at room temperature under high pressure

Hydrates C-S-H were studied by ^{29}Si NMR. NMR experiments show that no difference is visible in the C-S-H chain length. The product is similar to the product formed in normal conditions of temperature and pressure. However the kinetics of hydration depend a lot of pressure. Fig. 1 shows the conductivity curve of hydrating C_3S under 300 bar at room temperature. The different parts of the curve are well known [10]: the first increase of conductivity corresponds to C_3S dissolution, the peak to Porlandite precipitation, and the last step to the progressively connecting network. C_3S dissolution is accelerated by pressure, as presented on Fig. 2 and Fig. 3 which shows the comparison of hydration of C_3S under 300 bar and 850 bar during the first hydration hour. This pressure effects goes on during hydration. As shown in Fig. 4 the complete conductivity curve is affected by pressure: The porous network forms quicker under 850 bar (10 hours) as under atmospheric pressure (20 hours).

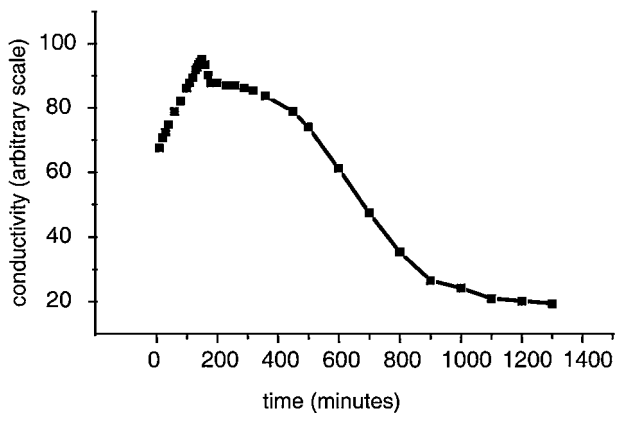

Figure 1 Conductivity curve of hydrated C_3S at normal temperature under 300 bar.

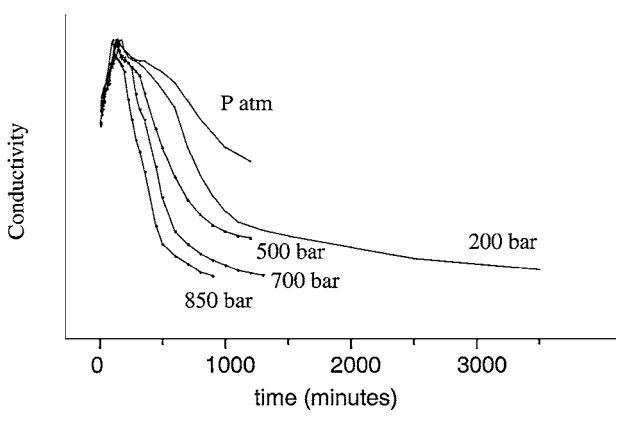

Figure 2 Conductivity curves of hydrated C_3S under different pressure.

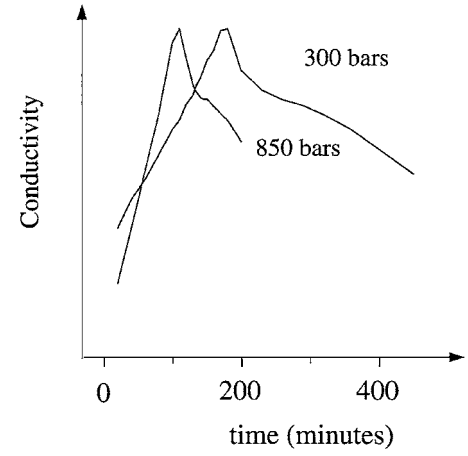

Figure 3 Conductivity of hydrated C_3S under 300 bar and 850 bar : C_3S dissolution step.

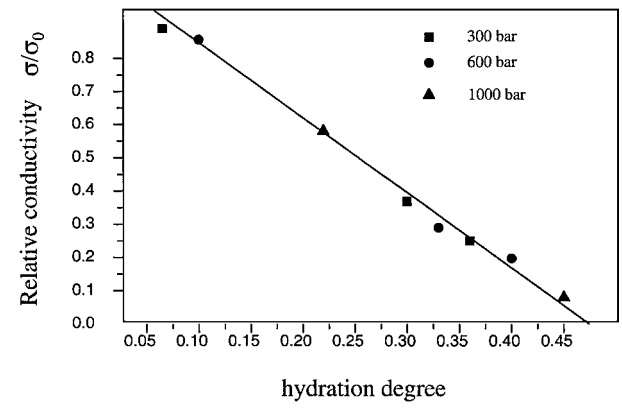

Figure 4 Relative conductivity (compared to conductivity when portlandite precipitates) versus hydration degree in the case of C_3S hydration without quartz for different hydration pressure at room temperature.

3.2. Hydration at 120°C

3.2.1. Characterization of hydrates formed under saturated steam pressure

Samples of C_3S hydrated with and without ground quartz during 1, 2 and 7 days were investigated by single pulse ^{29}Si NMR experiments and ^{1}H-^{29}Si cross polarization NMR experiments with varying contact time. As shown in Fig. 5, the spectra of C_3S hydrated at 120°C during 7 days with and without ground quartz are very similar. The peaks group between −68 ppm

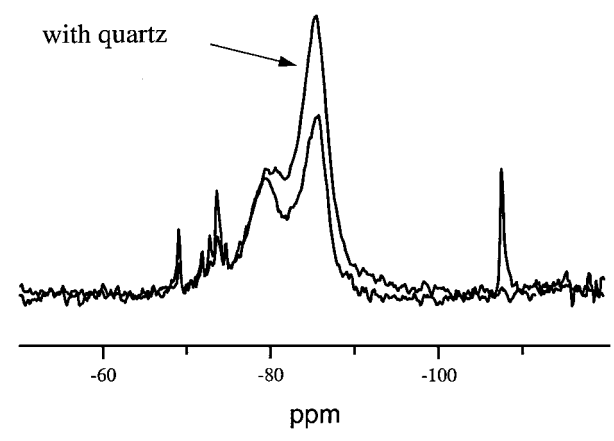

Figure 5 Superposition of ^{29}Si single pulse spectra of C_3S hydrated during 7 days with and without ground quartz under saturated steam pressure.

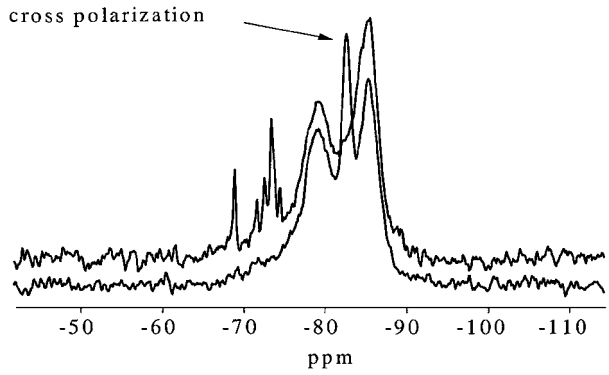

Figure 6 Superposition of ^{29}Si single pulse and ^{1}H-^{29}Si cross-polarization NMR spectra (contact time of 7 ms) of C_3S hydrated at 120°C under steam pressure during 7 days.

and −75 ppm corresponds to the non-hydrated C_3S, the two peaks located at −79.2 ppm and −85.5 ppm are attributed respectively to Q_1 and Q_2 resonance of the non-crystalline C-S-H and the fine peak located at −107.5 ppm is attributed to the quartz in the sample hydrated with quartz. These spectra clearly show that the silicate chains of the C-S-H hydrated in presence of quartz are much longer than in the case of hydration without quartz. The correlated effects of temperature and quartz addition on C_3S hydration are clearly observed on these spectra.

In order to study more precisely hydrates formed under these conditions, ^{1}H-^{29}Si cross-polarization experiments were acquired with varying contact time. Fig. 6 shows the comparison between a single pulse ^{29}Si NMR experiment and a ^{1}H-^{29}Si cross-polarization NMR experiment of C_3S hydrated at 120°C during 7 days. In the cross-polarization spectrum a narrow peak (−82.7 ppm) clearly appears which is not obviously observed on the single pulse spectrum. This peak is observed on each cross-polarization spectrum of C_3S hydrated with and without ground quartz at 120°C up to 7 days. Several attributions are possible. A varying contact time experiment allows to study the polarization dynamic of each resonance in the hydrated C_3S cross-polarization spectra. An example is given for C_3S hydrated during 7 days at 120°C (Fig. 7). The peak

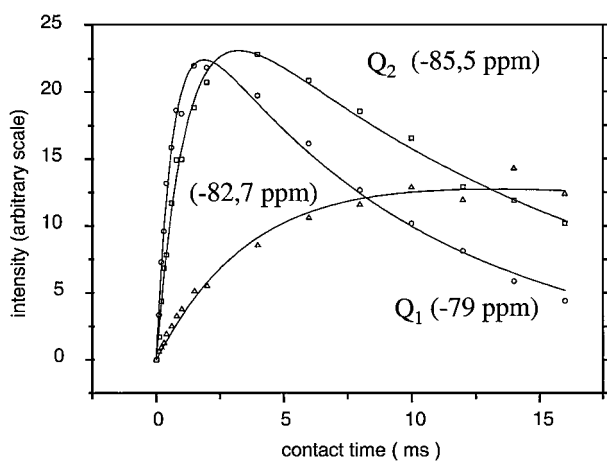

Figure 7 C_3S hydrated during 7 days at 120°C under steam pressure. Varying contact time ^{1}H-^{29}Si NMR experiment: Magnetization intensity versus contact time for each resonance of the cross-polarization spectrum.

located at −82.7 ppm has a particular dynamic, which is completely different from the other peaks dynamic and can be attributed to the tricalcium silicate hydrate or Jaffeite phase. This phase is evidenced by an X ray diffractogram of C_3S hydrated with and without ground quartz at 120°C. This Jaffeite phase was mentioned in a previous work in similar hydration conditions, and with the same observed chemical shift [21]. NMR is a good tool to highlight Jaffeite, which is very sensible to a long time cross-polarization experiment.

A combined X-ray diffractogram and thermal analysis yield to a rough estimation of each phase present in a sample of C_3S hydrated 2 days at 120°C without ground quartz: Jaffeite amount is estimated to 5% in oxide mass. The C-S-H [C]/[S] ratio can be in this case estimated to 2. A CRAMPS ^{1}H NMR study of hydration of C_3S hydrated in saturated steam pressure conditions at 120°C up to 7 days showed [21] that a lot of Ca—OH bond are present in C-S-H hydrates formed in these conditions even in a sample hydrated 7 days with ground quartz in which no Portlandite is detected by X-ray diffraction (area Si—OH/Ca—OH ratio equal to 1). This observation is coherent with a high C-S-H [C]/[S] ratio.

3.2.2. Hydration under high pressure

Early stage hydration (few hours up to few days) of C_3S with and without ground quartz under a pressure of 400 bar and 1000 bar were investigated by ^{29}Si NMR, ^{1}H CRAMPS NMR, ^{1}H-^{29}Si cross-polarization NMR, thermal analysis and quantitative Rietveld XRD (Fig. 8). The last technique is of practical interest for the study of phases as Jaffeite and α-C_2SH. However owing to the presence of non-well crystallised phases as C-S-H and problems of preferential orientation of Portlandite, the quantitative Rietveld results have to be carefully interpreted. These results can be seen as semi-quantitative. All the techniques are systematically compared: Portlandite amount obtained by thermal analysis is preferred to the amount obtained directly by Rietveld due to the preferred orientation. The combined results from XRD quantitative analysis and thermal analysis in the case of C_3S hydrated with and without ground quartz at 120°C under 400 bar and 1000 bar are displayed on Fig. 9. The deleterious α-C_2SH phase clearly

	Without quartz 400 bar	With quartz 400 bar	Without quartz 1000 bar	With quartz 1000 bar
C_3S	8%	6%	17%	10%
Quartz		15.5%		13.5%
Jaffeite	(6%) 8%		(3%) 3.5%	
CH	(21%) 16%		(18%) 15%	
α-C_2SH		(14.5)% 15%		(13%) 14%
CSH	63%	65.5%	62%	63%
[C]/[S]	2	1.5	2.1	1.5

Figure 8 C_3S hydrated with and without quartz under high pressure during 4 days. Combined results of Rietveld XRD and thermal analysis (results in brackets). Anhydrous phases are determined by Rietveld XRD. Jaffeite, Portlandite and α-C_2SH are determined by thermal analysis and Rietveld XRD. C-S-H is deduced from the knowledge of the other phases.

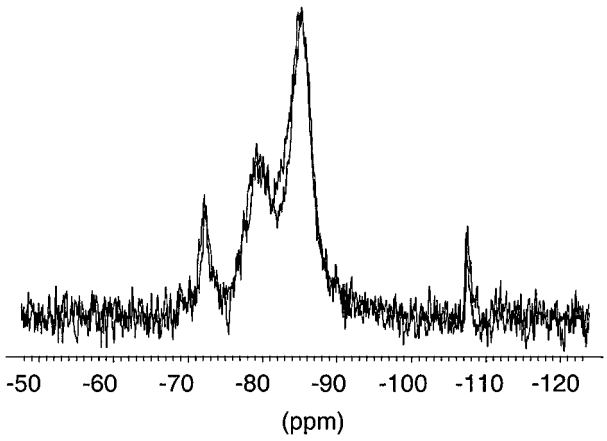

Figure 9 Superposition of single pulse ^{29}Si NMR spectra of C_3S hydrated with ground quartz during 4 days at 120°C under a pressure of 400 bar and 1000 bar. Both spectra seem to be quite identical.

appear under pressure influence when ground quartz is present (initial [C]/[S] ratio lowered). The known amount of each phase allows us to estimate the C-S-H [C]/[S] ratio in both cases: hydration with and without quartz. The C-S-H [C]/[S] ratio is roughly equal to 2 for hydration without quartz and 1.6 for hydration with quartz. The amounts of each phase determined by thermal analysis and Rietveld XRD are approximately equal except for Portlandite: XRD results are underestimated in comparison with thermal analysis. These observations are qualitatively confirmed by NMR experiments. As shown on the Fig. 10, single pulse ^{29}Si NMR spectra of C_3S hydrated with quartz at 120°C during 4 days under a pressure of 400 bar and 1000 bar (Fig. 11) are quite identical. The resonance located at −72 ppm is due to the α-C_2SH [22, 23] and the one located at −107.5 ppm is due to the quartz. A ^{1}H-^{29}Si cross-polarization spectrum (acquired with a 10 ms contact time) of C_3S hydrated with quartz at 120°C during 4 days under a pressure of 1000 bar exhibits a large peak corresponding to the α-C_2SH phase and a small due to the Jaffeite (Fig. 12). This result indicates that a small amount of Jaffeite is present in the mixture (cross-polarization is very sensible to presence

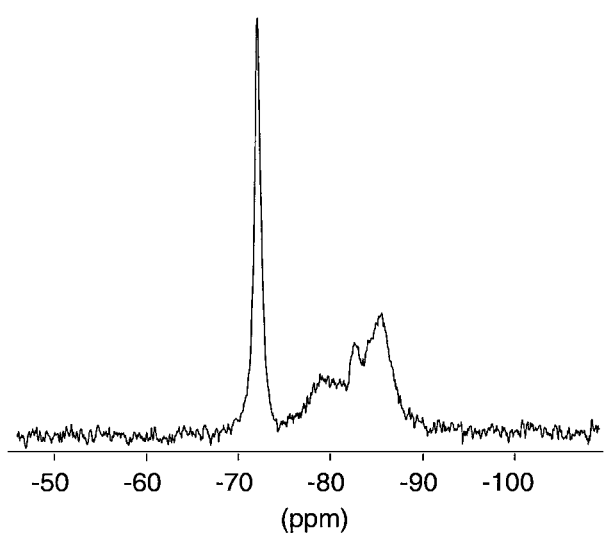

Figure 10 ^{1}H-^{29}Si cross polarization (10 ms contact time) NMR spectrum of C_3S hydrated with quartz at 120°C during 4 days under 1000 bar.

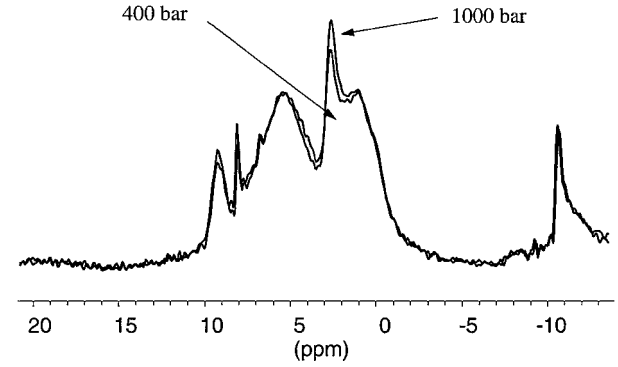

Figure 11 Superposition of ^{1}H CRAMPS NMR spectra of C_3S hydrated with quartz during 4 days at 120°C under a pressure of 400 bar and 1000 bar.

	Steam pressure	400 bar	800 bar	1200 bar
16 hours		CH : 9% Jaffeite : 27% C_3S : 7.5% C-S-H : 56.5% [C]/[S] = 2.4	CH : 11.5% Jaffeite : 26% C_3S : 9% C-S-H : 54 [C]/[S] = 2.3	
1 day		CH : 20% Jaffeite : 4.5% α-C_2SH : 34% C-S-H : 40% [C]/[S] = 2.2		CH : 15% Jaffeite : 8% α-C_2SH : 46% C-S-H : 30%
4 days	CH : 12% Jaffeite : 20% C_3S : 7% α-C_2SH : 4% C-S-H : 56% [C]/[S] = 2.2			CH : 17% Jaffeite : 10.5% α-C_2SH : 44% C-S-H : 30% [C]/[S] = 2.3

Figure 12 C_3S hydrated without quartz at 160°C under pressure from steam pressure up to 1200 bar during few hours to few days. Proportions are determined by Rietveld XRD except Portlandite, which is determined by thermal analysis.

	400 bar	800 bar	1000 bar
16 hours	Quartz : 13% Jaffeite : 15.5% C-S-H : 71.5% [C]/[S] = 1.5	Quartz : 14.5% α-C_2SH : 33.5% Jaffeite : 5.1% C-S-H : 47% [C]/[S] = 1.6	
30 hours	Quartz : 10.5% α-C_2SH : 17.5% Jaffeite : 5% C-S-H : 67% [C]/[S] = 1.2	Quartz : 12% α-C_2SH : 16.5% Jaffeite : 7.5% C-S-H : 63.5% [C]/[S] = 1.4	
65 hours	Quartz : 14% α-C_2SH : 58% C-S-H : 28% [C]/[S] = 1.2	Quartz : 12% α-C_2SH : 47% C-S-H : 40.5% [C]/[S] = 1.2	
11 days			Quartz : 12% α-C_2SH : 47.5% C-S-H : 41% [C]/[S] = 1.2

Figure 13 C_3S hydrated with quartz at 160°C under pressure during few hours up to few days. Proportions are determined by XRD Rietveld and thermal analysis.

of Jaffeite) and that α-C_2SH is also evidenced by high contact time in cross-polarization. On the Fig. 13 is displayed the superposition of ^{1}H CRAMPS NMR spectra of C_3S hydrated with quartz at 120°C during 4 days

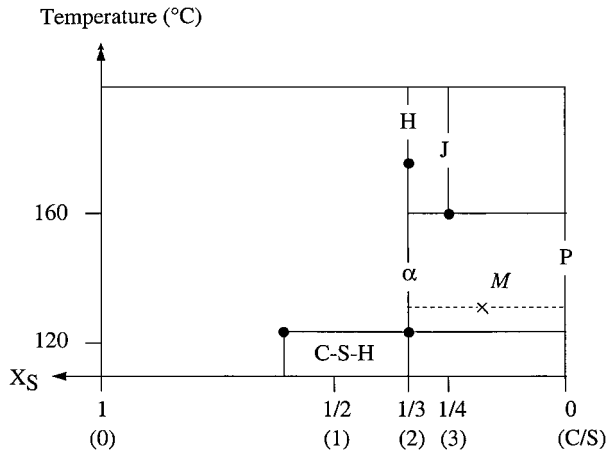

Figure 14 Phase diagram [C]/[S]-temperature at saturated steam pressure. The *X* axis unit is molar fraction X_s (The corresponding [C]/[S] ratio is in bracket) and the *Y* axis is the temperature. $\alpha = \alpha$-C_2SH, J = Jaffeite, P = Portlandite, H = Hillebrandite. As an example, M is a mixture of α-C_2SH and Portlandite with a global [C]/[S] ratio between 1/4 and 0.

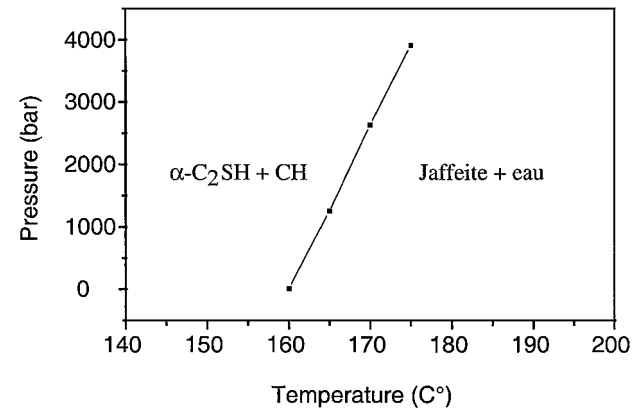

Figure 15 $P(T)$ variation curve of equilibrium between Portandite + α-C_2SH and Jaffeite + water.

under 400 bar and 1000 bar. The spectra clearly exhibits peaks due to α-C_2SH [24] (peaks located at 9.2 ppm and 2.4 ppm) and the large peak due to the C-S-H. The high Ca—OH content is coherent with a high [C]/[S] ratio obtained even with a hydration with quartz. The resonance peak located at 8 ppm can be displaced when changing the irradiation frequency or speed rotation: this peak is an artefact.

3.3. Hydration at 160°C

As in the previous case, Rietveld and thermal analysis were compared to obtain the amount of each phase. Thermal analysis was used for Portlandite analysis because of the preferred orientation. Portlandite and α-C_2SH cannot be distinguished by thermal analysis. However it is possible to study the global thermal signal and compare XRD to thermal analysis. The Fig. 14 displays the results obtained by these two techniques in the case of hydration of C_3S at 160°C under pressure without quartz during few hours up to few days. Jaffeite tends to disappear under pressure effect while α-C_2SH increases with hydration time. This effect seems to be less effective at saturated steam pressure. In the case of hydration of C_3S with quartz, no correction is done with thermal analysis due to the absence of Portlandite. Thermal analysis is used in order to confirm the amounts determined by XRD. Fig. 15 presents the results obtained for C_3S hydration with quartz at 160°C under pressure between a few hours and a few days. Jaffeite clearly tends to disappear in favour of α-C_2SH with increasing pressure. These observations are qualitatively confirmed by ^{29}Si NMR spectra.

4. Discussion

4.1. NMR contribution to high temperature C-S-H structure

^{29}Si NMR experiments show that the temperature increases the length of the C-S-H silicate chains. However, the solid [C]/[S] ratio of C-S-H formed at high temperature is high (roughly close to 2) even in a case of hydration with ground quartz. In various studies, correlations have been done between [C]/[S] ratio and chain length determined by NMR showing that low [C]/[S] ratio correspond to long chain length [1]. This biunivoque relation is valid only at a fixed temperature and the chain length of C-S-H depends on temperature as well as [C]/[S] ratio in solution (modified by presence of quartz) which are decorrelated parameters.

Decompositions have been done in order to interprete the spectra. The structural model of C-S-H is based on dreierketten pattern (Tobermorite structure) of the silicate chain [25, 26] where two paired tetrahedra for one bridging tetrahedron appear. NMR studies shows that bridging tetrahedron can be assigned to a reasonance around −82 ppm and the paired around −85.5 ppm in C-S-H of low [C]/[S] ratio or in synthetic Tobermorite [27]. In this study, in spite of the difficulties arousing from bad signal/noise ratio and non-completely resolved spectra, it is difficult—for the spectra of C_3S hydrated without ground quartz—to find a decomposition in which these two Q_2 peaks appear. However, there is a non-unique possible solution with a peak at −84 ppm and a peak at −85.5 ppm with a ratio of the two peaks equal to 2, according to a dreierketten pattern. The decomposition of spectra of C_3S hydrated with ground quartz need a component around −82 ppm. This would be coherent with the hypothesis of Tobermorite-like structure for C-S-H with low [C]/[S] ratio even at high temperature. But no evidence is given for high [C]/[S] ratio and the peak at −84 only appear as a clue.

4.2. Phase diagram

The aim of this discussion is to propose a model, which allows to understand the hydrating system under high pressure. An X_s-Temperature (where X_s stands for Silicon molar fraction) binary diagram is first drawn at saturated steam pressure. Several hypothesis are needed to draw this diagram: 160°C corresponds to the minimum temperature of Jaffeite stability. Under this temperature, the mixture Portlandite + α-C_2SH is stable. The upper limit of C-S-H stability is above 120°C. The upper limit of α-C_2SH stability is above 160°C. The Fig. 16 present the phase diagram under saturated steam pressure in the range of high [C]/[S] ratio. The two equilibria at saturated steam pressure under interest are the following:

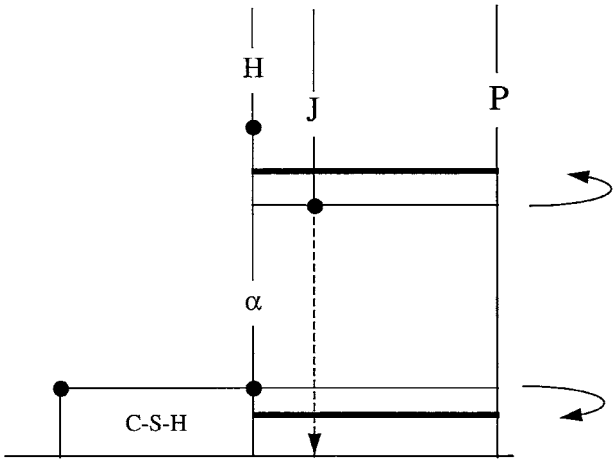

Figure 16 Equilibrium lines for equilibrium (1) and (2) are displaced under pressure effect (1000 bar).

at 160°C

$$C_3SH_{1.5}(\text{Jaffeite}) + 0{,}5H_2O \rightarrow \alpha\text{-}C_2SH + CH \quad (1)$$

at 120°C

$$C_p{-}S{-}H_q{+}(2{-}p)CH \rightarrow \alpha\text{-}C_2SH{+}(q{+}1{-}p)H \quad (2)$$

The q and p coefficients are respectively C-S-H [C]/[S] ratio and H/S ratio.

According to phase rule, a variance of 1 allows three solid phases to coexist and the temperature is linked to the pressure. In the case of equilibria (1) and (2), $P(T)$ curve can be calculated. Using the thermodynamic relation $\Delta_r G_i^o = -RT \ln K$, where K stands for equilibrium constant of the reaction and i indice stands for the components involved in the reaction. The first term of equation $\Delta_r G^o$ refers to a standard state, which has to be chosen. Standard temperature and standard pressure can in particularly be chosen equal to temperature and pressure of the system [28]. In this case, equilibrium constant depends on P and T and the $P(T)$ equilibrium curve is determined by equation $\ln K = 0$ corresponding to an equilibrium state. Variation of $\ln K$ with temperature and pressure can be calculated from the relations [28]:

$$\frac{\partial}{\partial T}(RT\ln K) = \frac{\partial}{\partial T}\left(-\Delta_r G^o/T\right) = \Delta_r H^o/T^2 \quad (A)$$

and

$$\frac{\partial}{\partial P}(\ln K) = \frac{-1}{RT}\frac{\partial}{\partial P}\left(\Delta_r G^o\right) = \frac{-1}{RT}\left(\Delta_r V^o\right) \quad (B)$$

In the first expression, P is kept constant, and in the second, T is kept constant. These expressions mean that standard enthalpy and standard volume change of reaction determines the rate of K variation. The volume term $\Delta_r V^o$ as enthalpy term $\Delta_r H^o$ depends on pressure and temperature. However, when $\Delta_r V^o$ corresponds to incompressible phases, $\Delta_r V^o$ is a constant and the variation of $\ln K$ reduces to the term $-1/RT\,\Delta_r V^o$. In the other case (fluid compressible phase involved), a water equation state is necessary to take account of variation of molar volume with pressure. This difference of molar volume $\Delta_r V^o$ is directly determined from the knowledge of the density of each phases. In the case of equilibrium (1) and (2) described before, $\Delta_r H^o$ can be estimated by a phenomenological law [29] of formation enthalpy of each silicate [30].

$$\Delta_f H^o(C_1S_mH_n) = 1\Delta_f H^o_{\text{Portlandite}} + m\left(\Delta_f H^o_{\text{quartz-}\beta} + 6.0\text{ kcal}\right) + (n-1)\Delta_f H^o_{\text{liquidwater}}$$

The dependence of this enthalpy term with temperature can be estimated by the knowledge of calorific capacities of each phase, expressed as a function of Maier-Kelley coefficients [30]. In this study, this correction in calculation is neglected and eventually does not affect the conclusions of the study. In the $\Delta_r V^o$ calculation, the water-gas contribution and liquid-water contribution has to be introduced [31]. The incompressibility of liquid water is assumed. As mentioned above, Equations A and B allow to calculate $\ln K$ for a couple (T, P): equilibrium curve is determined by searching, for a given value of T, the value of P which yield to $\ln K = 0$. The Fig. 17 shows the calculation results as a $P(T)$ curve of (1) equilibrium between Jaffeite and α-C_2SH + Portlandite. The linear pressure dependence of pressure versus temperature is to incompressibility of the phases, especially water. Under pressure effect, the α-C_2SH formation is favoured at a fixed temperature of 160°C. The same calculation can be done for the (2) equilibrium between C-S-H and α-C_2SH + Portlandite. The main problem with this calculation is related to C-S-H density evaluation. In the case of a density of C-S-H equal to 1.9 [32] the calculation yield to a negative value of $\Delta_r V^o$. The equilibrium temperature is then lowered when pressure increases. A summary of these results is shown on Fig. 18. The diagram C-S-temperature under saturated pressure and under 1000 bar is superposed.

4.3. Time evolution of the system under high temperature and high pressure

4.3.1. Room temperature

At room temperature, the pressure has no effect on the hydrates structure. However, an important kinetics effect can be observed. As in the case of equilibrium temperature change with pressure, kinetics effect of pressure can be explained in term of molar volume differences [33]. Theoretically, a reaction kinetic defined by factor k has the following pressure dependence:

$$\frac{\partial RT\ln k}{\partial p} = -\Delta V^{\ddagger}$$

where $\Delta V^{\ddagger}$ stands for the "activated complex" or intermediate product of reaction. The volume term is negative for hydration under pressure. The experimental part showed that the pressure affect the kinetic hydration (both dissolution and precipitation when network is forming). However, it is not known if the pressure effect is only kinetics or if it affects the network. The Fig. 4 shows the relative conductivity (measured conductivity divided by conductivity at the precipitation

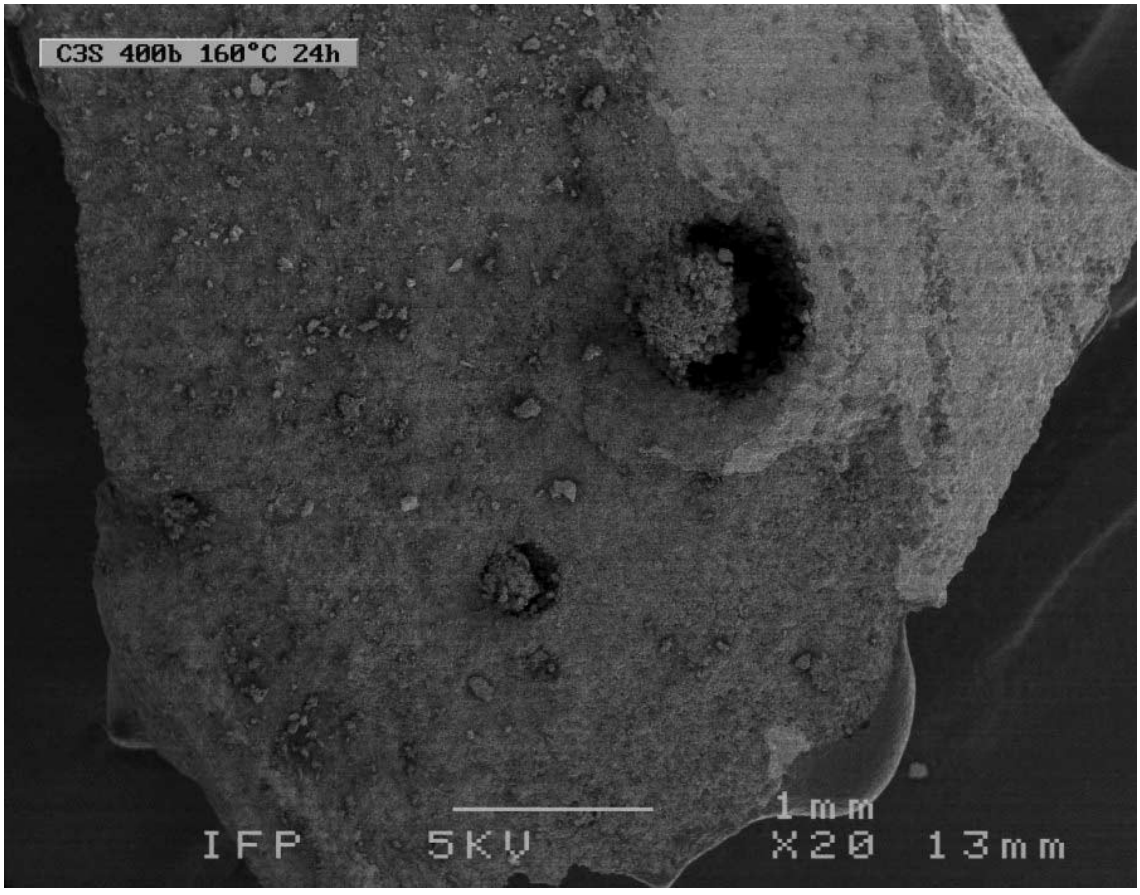

Figure 17 SEM Photographs. C_3S hydrated under 400 bar at 160°C during 24 hours (* 20). Two areas can be distinguished clear and dark.

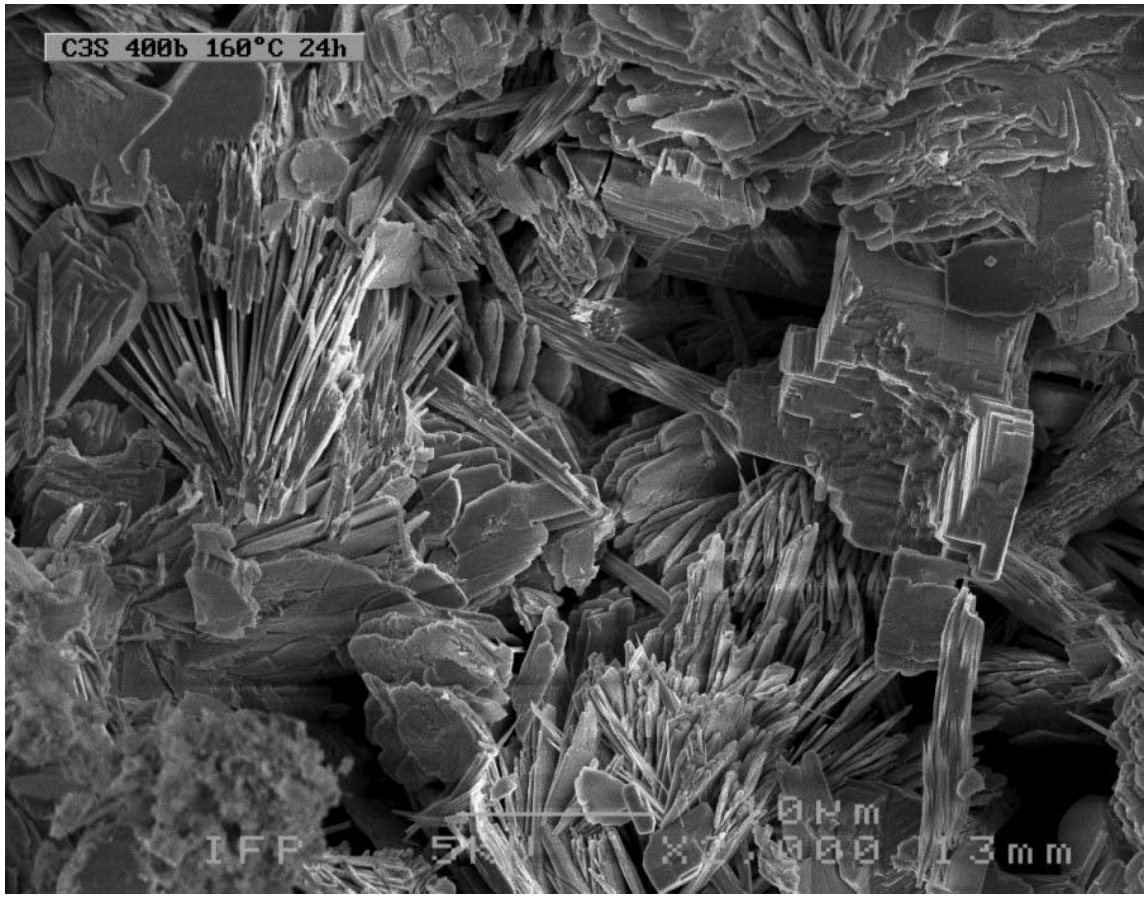

Figure 18 SEM photographs. C_3S hydrated under 400 bar at 160°C during 24 hours (* 2000). Dark region.

of Portlandite) of a hydrating sample versus hydration degree at room temperature under different pressure. All the points seem to be on a unique curve, indicating that the effect of pressure, at least in the first stage of hydration, is only kinetics: the paste state depends on the hydration degree, which depends on the pressure.

4.3.2. Hydration under 160°C

In the case of hydration at 160°C, phase diagram introduced previously is helpful for interpretations. The two cases with and without quartz can be studied separately.

4.3.2.1. Hydration without quartz. Experiments at 160°C tend to show that C-S-H is the first product formed, then Jaffeite and eventually α-C_2SH. This series of reactions tends to be quicker as pressure increases. Two explanations are possible: the first is due to equilibrium modification and the second is kinetic. Both cases are described and both are linked to a difference of molar volume between components.

The situation at saturated steam pressure is first examined. The representative point of the system, defined by the temperature equal to 160°C and the global [C]/[S] equal to 3, can be plotted on the phase diagram at saturated steam pressure. The equilibrium situation described by the phase diagram in these conditions indicates an equilibrium between three phases Jaffeite, α-C_2SH and Portlandite only. During C_3S hydration, even at high temperature, C-S-H is the first product formed (this amorphous product is the easiest to form) with a high [C]/[S] ratio (close to 2) because the global [C]/[S] of the system is equal to 3. The system is out of equilibrium because phase's rule is not respected and C-S-H is not stable at this temperature. According to the proposed phase diagram, two reactions can take place to explain the decrease of C-S-H with hydration time:

(1) C-S-H (high [C]/S] ratio) + CH → Jaffeite + water

(2) C-S-H (high [C]/S] ratio) → α-C_2SH + water

The second reaction can involve CH formation depending on the C-S-H [C]/[S] ratio. The system evolves in such a way that all C-S-H phase should vanish in benefit to crystalline phases. However, these reactions are limited by the available water and the final products will eventually depend on initial water content in the paste.

The high-pressure diagram shows that the equilibrium temperature between Jaffeite, CH and α-C_2SH is removed by pressure effect (5 degrees per 1 Kbar). At high pressure, the representative point of the system (160°C, [C]/[S] = 3) plotted on a high-pressure diagram is in a region of stability of α-C_2SH + CH at the difference with the precedent situation. During a high-pressure hydration at 160°C, C-S-H phase is the first hydrate formed, then Jaffeite and α-C_2SH. Jaffeite is easily formed because its [C]/[S] ratio is equal to the solution [C]/[S] ratio. However, the system can reach equilibrium through the following reactions:

(3) C-S-H → α-C_2SH if C-S-H [C]/[S] ratio is close to 2

(4) Jaffeite → α-C_2SH + CH

Higher the pressure, the more efficient is the return to equilibrium. This has been explained by the difference in molar volume between the components Jaffeite and CH + α-C_2SH. However, at normal temperature, it has been shown that effects the kinetics of reactions. This kinetics can also be related to a difference in molar volume called activation volume [33]. If precipitation of ionic solution can yield to Jaffeite or α-C_2SH + CH mixture, pressure will favor the phases with lower molar volume. In this case, the difference of molar volume between Jaffeite and α-C_2SH + CH yields to a quicker formation of α-C_2SH than Jaffeite.

This analysis is supported by the microscopy photographs. Fig. 17 shows a photograph of C_3S hydrated during 24 hours under 400 bar at 160°C. Two distinct areas are displayed: a clear region and a dark region, which are both displayed in Fig. 18 and Fig. 19, the latter with a greater view. It is shown that the clear region is a mixture of C-S-H and Portlandite where no other crystals appear. In this region, the phase's rule is locally respected but C-S-H is not a stable phase at this temperature. The dark region is more porous and is a mixture of Portlandite, α-C_2SH (with a characteristic fan-shaped morphology) and C-S-H. The macroscopic system, out of equilibrium, is highly heterogeneous and formed by regions assemblage (1 mm^3 typically) more homogeneous: porous crystalline regions and compact C-S-H regions. The system, initially a mixture of C-S-H and portlandite is returning to equilibrium by forming a region of increasing size where C-S-H disappear while more stable crystals like α-C_2SH appear. In this region, the phase's rules is not respected because the system is out of equilibrium and C-S-H is dissolving. Depending on the available water, the system evolution yields to an increase of crystalline regions.

4.3.2.2. Hydration with quartz. The situation is more complicated if quartz is present. Non-equilibrium has two origins: early-formed products are not stable (like C-S-H) and the difference of dissolution kinetics between C_3S and quartz yields to [C]/[S] ratio gradients in solution which depend on hydrating time. The system can be roughly separated in two steps: first, C_3S particles hydrates with inactive quartz particles, then, quartz dissolves. During the first step (C_3S hydration), the system is similar to the one described before: the system is first out of equilibrium because of high [C]/[S] ratio C-S-H and Jaffeite formation, whatever the pressure. The system reaches the equilibrium according to reactions (1) and (2) which describes hydration under saturated steam pressure and hydration under high-pressure respectively. However these reactions are completed by pozzolanic reaction due to quartz activity: [C]/[S] ratio in solution is lowered and the equilibrium can be reached by reactions:

Quartz + CH → C-S-H with low [C]/[S] ratio

C-S-H with low [C]/[S] ratio is not stable and should disappear but on the time scale that was studied, no experiment could evidence such a reaction.

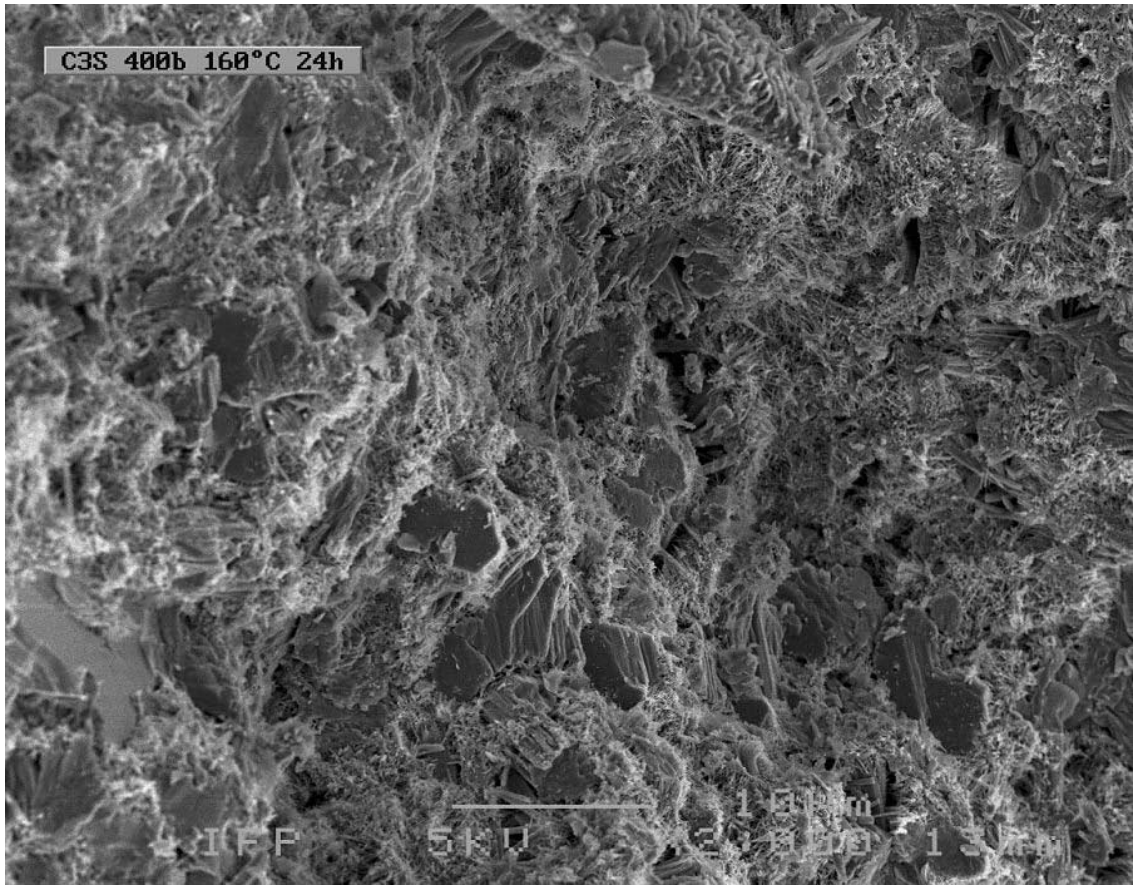

Figure 19 SEM photographs. C_3S hydrated under 400 bar at 160°C during 24 hours (* 2000). Clear region.

4.3.3. Hydration under 120°C

In the case of hydration without quartz, hydration is clearly explained by the phase diagram: the diagram at saturated steam pressure at 120°C, in the case of [C]/[S] ratio equal to 3, forecasts an equilibrium between C-S-H and Portlandite and the diagram at high pressure yields to the same mixture, because it has been assumed that the equilibrium temperature between C-S-H + CH and α-C_2SH was above 120°C, whatever the pressure. However, equilibrium temperature is slightly lowered by pressure effect.

In the case of hydration with quartz, hydration should yield to C-S-H with [C]/[S] ratio, whatever the pressure, according to the previous assumptions. Formation of α-C_2SH could be explained by a kinetics factor: as in the case of hydration at 160°C, the difference of molar volume can change kinetics of reaction.

5. Conclusion

Pressure (1000 bar) and temperature (160°C) effects on C_3S hydration in paste with and without ground quartz have been investigated in this study. At room temperature, C_3S hydration kinetic is increased by pressure. Dissolution is activated: increase of conductivity corresponding to C_3S dissolution is faster under pressure so that Portlandite precipitation occurs earlier. Precipitation process is also activated: hydrates (C-S-H + Portlandite) precipitation is faster under pressure so that the network forms more rapidly under pressure. The drawing of conductivity versus hydration degree for different hydration pressure shows that pressure effect at room temperature seems to be only kinetic. This process can be explained in term of activation volume. The C-S-H structure at room temperature does not seem to be changed by the pressure only as shown by XRD and NMR analysis. However, properties like water content of C-S-H have not been investigated.

C_3S hydration at higher temperature (up to 160°C) yields to hydrates different from those formed at room temperature. The crystalline phases Jaffeite and α-C_2SH appear during C_3S paste hydration, more stable than C-S-H at a temperature above 120°. However, C-S-H always is the first hydrate formed and its structure depends on hydration temperature. At room temperature, the chain length is strongly correlated to C-S-H [C]/[S] ratio (C-S-H with low [C]/[S] ratio have a Tobermorite-like structure with quite high silicate chain length while high [C]/[S] ratio C-S-H have short chains). The temperature modifies this property and it is possible to form C-S-H with high [C]/[S] ratio and quite long silicate chain (in comparison with C-S-H obtained at room temperature).

In this study, a phase diagram, which helps to understand the chemical reaction sequence, has been built, according to rules phase. Owing to time scale of experiments and equilibrium concept, this diagram allows to consider the hydrates formed (in particular α-C_2SH and C-S-H) as equilibrium phases. The pressure displacement of equilibrium temperature for each equilibrium has been calculated on thermodynamical basis and compared with experiment results. The pressure

dependence of equilibrium temperature can be described (as for the kinetic constant) by an activation volume, which depends itself on molar volume of each component. Water contribution has to be introduced. When dealing with incompressible phases, the equilibrium temperature dependence is linear as in the case of equilibrium between Jaffeite, α-C_2SH and Portlandite. The pressure dependence of equilibrium temperature is quite weak: 5 degree per 1000 bar typically. This thermodynamic tool allows us to have a critical look on the curve shape given in the literature. In particular, in the case of Portlandite de-hydration [8], the horizontal curve shape in the low temperature domain is clearly explained by a compressible water-fluid contribution allowed by the fact that de-hydration occurs above the water critical point.

Better treatment of pressure and temperature hydration thermodynamic should probably take into account the crystal growth, which could modify the equilibrium relations because of the size of crystals.

References

1. H. F. W. TAYLOR, in "Cement Chemistry" (Thomas Telford, London, 1997) p. 113.
2. I. HARKER, *J. Amer. Ceram. Soc.* **47** (1964) 521.
3. E. R. BUCKLE and H. F. W. TAYLOR, *J. Appl. Chem.* **9** (1959) 163.
4. I. ODLER, *J. Appl. Chem. Biotechnol.* **23** (1973) 661.
5. S. MASSE, H. ZANNI, J. LECOURTIER, J. C. ROUSSEL and A. RIVEREAU, *J. Chim. Phys.* **92** (1995) 1861.
6. D. M. ROY and R. I. HARKER, in Proceedings of the 4th International. Symposium on Chemistry of Cement (1962) Vol. 1, p. 196.
7. D. M. ROY and A. M. JOHNSON, in Proceedings of the Symposium on Autoclaved Calcium Silicate Building Products (1967) p. 114.
8. C. W. F. T. PISTORIUS, *American Journal of Science* **261** (1963) 79.
9. H. F. W. TAYLOR, in Proceedings of the 5th International Symposium on Chemistry of Cement, Session II-1 (1968) p. 1.
10. C. VERNET and G. NOWORYTA, in Proceedings of the 9th International Congress on the Chemistry of Cement, New Delhi, 1992 (National Council for Cement and Building Materials, 1992) p. 627.
11. B. J. CHRISTENSEN, T. O. MASON and H. M. JENNINGS, *J. Amer. Ceram. Soc.* **4** (1992) 939.
12. J. C. TATLOR and L. P. ALDRIDGE, *Powder Diffraction* **3** (1993) 138.
13. S. MANSOUTRE and N. LEQUEUX, *Adv. Cem. Res.* **8** (1996) 175.
14. N. I. GOLOVASTIKOV, R. G. MATVEEVA and N. V. BELOV, *Sov. Phys. Crystallogr.* **20** (1975) 441.
15. J. FAYOS and M. PEREZ-MENDEZ, *Am. Ceram. Soc. Bull.* **8** (1986) 1191.
16. L. HELLER, *Acta Cryst.* **5** (1952) 724.
17. R. E. MARSH, *ibid.* **C50** (1994) 996.
18. N. YAMNOVA, C. H. SARP, Y. K. EGOROV-TISMENKO and D. Y. PUCAROVSKY, *Kristallographia* **38** (1993) 73.
19. X. CONG and R. J. KIRKPATRICK, *Adv. Cem. Res.* **7** (1995) 103.
20. A. R. BROUGH, C. M. DOBSON, I. G. RICHARDSON and G. W. GROVES, *J. Mater. Sci.* **29** (1994) 3926.
21. B. BRESSON, H. ZANNI, S. MASSE and C. NOIK, *ibid.* **32** (1997) 4633.
22. G. M. M. BELL, J. BENSTED, F. P. GLASSER, E. E. LACHOWSKI, D. R. ROBERTS and M. J. TATLOR, *Adv. Cem. Res.* **3** (1990) 23.
23. A. R. GRIMMER, in Application of NMR Spectroscopy to Cement Science, Guerville, March 1992, edited by P. Colombet and A. R. Grimmer (Gordon & Breach, Paris, 1994) p. 113.
24. D. HEIDEMANN, in Application of NMR Spectroscopy to Cement Science, Guerville, March 1992, edited by P. Colombet and A. R. Grimmer (Gordon & Breach, Paris, 1994) p. 77.
25. S. A. HAMID, *Zeitschrifüt für Kristallographie* **3** (1981) 189.
26. X. CONG and R. J. KIRKPATRICK, *Adv. Cem. Bas. Mat.* **3** (1996) 144.
27. I. KLUR, B. POLLET, J. VIRLET and A. NONAT, in Nuclear Magnetic Resonance Spectroscopy of Cement-Based Materials, Bergamo, June 1996, edited by P. Colombet, A. R. Grimmer, H. Zanni and P. Sozzani (Springer-Verlag, Berlin, 1998) p. 119.
28. G. ANDERSON and D. CRERAR, in "Thermodynamics in Geochemistry, the Equilibrium Model" (Oxford University Press, New-York, 1993) p. 269.
29. R. DRON and V. WALLER, in Nuclear Magnetic Resonance Spectroscopy of Cement-Based Materials, Bergamo, June 1996, edited by P. Colombet, A. R. Grimmer, H. Zanni and P. Sozzani (Springer-Verlag, Berlin, 1998) p. 227.
30. V. I. BABUSHKIN, G. M. MATVEYEV and O. P. MCHEDLOV-PETROSSYAN, in "Thermodynamics of Silicates" (Springer-Verlag, Berlin, 1985).
31. R. C. REID and T. K. SHERWOOD, in "The Properties of Gases and Liquids" (McGraw–Hill, London, 1966).
32. H. F. W. TAYLOR, in "Cement Chemistry" (Thomas Telford, London, 1997) p. 122.
33. R. S. BRADLEY, in "High Pressure Physics and Chemistry" (Academic Press, London, 1963).

Received 30 August 2000
and accepted 28 November 2001